Renewable Energy 36 (2011) 1728–1733

Contents lists available at ScienceDirect

Renewable Energy

journal homepage: www.elsevier.com/locate/renene

Design and performance of a moderate temperature difference Stirling engine

Angkee Sripakagorn*, Chana Srikam

Department of Mechanical Engineering, Faculty of Engineering, Chulalongkorn University, Phaya Thai Road, Wang Mai, Pathum Wan, Bangkok 10330, Thailand

ARTICLE INFO

Article history:
Received 1 July 2010
Accepted 11 December 2010
Available online 3 January 2011

Keywords:
Stirling engine
Concentrating solar power
Distributed generation
Solar energy
Parabolic trough

ABSTRACT

The present work developed a prototype Stirling engine working at the moderate temperature range. This study attempts to demonstrate the potential of the moderate temperature Stirling engine as an option for the prime movers for Concentrating Solar Power (CSP) technology. The heat source temperature is set to 350–500 °C to resemble the temperature available from the parabolic trough solar collector. This moderate temperature difference allows the use of low cost materials and simplified mechanical designs. With the consideration of local technological know how and manufacturing infrastructure, this development works with a low charged pressure of 7 bar and uses air as a working fluid. The Beta-type Stirling engine is designed and manufactured for the swept volume of 165 cc and the power output of 100 W. The performance of engine is evaluated at different values of charge pressures and wall temperatures at the heater section. At 500 °C and 7 bar, the engine produces the maximum power of 95.4 W at 360 rpm. The thermal efficiency is 9.35% at this maximum power condition. Results show that the moderate temperature operation offers a clear advantage in terms of the specific power over the low temperature operation. In terms of the West number, the present work demonstrated that the moderate temperature difference operations could offer the performance on par with the high temperature operations with more simple and less costly development.

© 2010 Elsevier Ltd. All rights reserved.

1. Introduction

Presently, the situation of electricity production consists of central power plants and distributed generation systems. For either case, renewable energy resources is one of the solutions to reduce the dependency on petroleum import, to increase the energy efficiency and to avoid the confrontations or conflicts usually arisen from the building of new large power plants based on fossil fuel. Undeniably, for a tropical country such as Thailand, solar energy is the renewable energy resources with the largest potential [1]. There is, however, a huge gap between the technical potential and the practical utilization of solar energy. According to the Ministry of energy of Thailand, the target for solar energy use in 2011 is a mere 45 MW from the present accumulated installation of 30 MW. One of the reasons behind the stagnant growth of solar energy utilization is the limitation of technological options. Presently, the technologies to harvest solar energy are rather limited to photovoltaic systems. The recent commercial successes in Europe and Mediterranean, however, have brought attentions to another option namely the solar thermal technologies or Concentrating Solar Power (CSP) [2–4]. On a smaller scale, the choices of the prime movers currently under development for CSP installations that generate from 1 to 100 kW of electricity include the Rankine cycle [5], the organic Rankine cycle [6–10] and the Stirling engine [11,12].

The present study focuses on the Stirling engine development. There are two major directions of the Stirling engine development; the high temperature and the low temperature designs. The high temperature design represents the benchmark for the solar-to-electricity conversion efficiency at 29.4%. Nevertheless, it comes at the cost that can be as high as 10,000 $/kW compared to 3000$/kW for the photovoltaic systems [2,12]. In contrary, the low temperature designs are currently developed to harness the low-grade heat at low cost [13–17]. However, the low temperature difference makes the efficiency and the specific power very small compared to the high temperature design. These limitations make it difficult for the low temperature design to work with the solar collectors while resulting in a reasonably modular and less costly installation. This work proposes that the moderate temperature is where the balance is. The higher efficiency and the specific power compared to the low temperature design allow a reduction in the cost of the solar field. The moderate temperature avoids the expensive alloys and complex design required in the high temperature design hence brings down the cost. This is in line with Tlili [22] who indicated that, to be competitive in small scale generations, Stirling engine working with average concentration ratio is the optimum choice. With 1-axis tracking parabolic trough, the operating temperature is

* Corresponding author. Tel.: +662 2186595; fax: +662 2522889.
E-mail address: angkee.s@gmail.com (A. Sripakagorn).

0960-1481/$ – see front matter © 2010 Elsevier Ltd. All rights reserved.
doi:10.1016/j.renene.2010.12.010

typically 300–390 °C [23] where the maximum temperature up to 550 °C is in commercial development [24].

There are few research works in the moderate temperature range. Kongtragool and Wongwises [17] demonstrated the performance of gamma-type Stirling engines with single-acting, twin power piston and four power pistons. The maximum power output reached 32.7 W for the four power piston version at 500 °C heater temperature under atmospheric pressure. Ishiki [18] studied on the atmospheric Beta-type Stirling engine using a pin-fin array heat exchanger. The engine yielded 91 W shaft output at 362 °C heater temperature. Karabulut [20,21] mentioned the limitations on the weight and volume the Rhombic drive placed on the solar dish application based on Stirling engines. They proceed to investigate the performance of the Beta-type Stirling engine based on a novel lever-controlled mechanism. The maximum power output is 183 W using helium at a moderate 4 bar charge pressure with no separate regenerator used.

The present work describes the design and construction of a Stirling engine developed for the moderate temperature range (350–500 °C). The engine prototype is experimentally evaluated such that the potential of the moderate temperature Stirling engine can be demonstrated. The performance of the engine is compared with results from related studies.

2. Design

The aim of this work directs toward the moderate temperature difference design. The hot end temperature is thus designed between 350 and 500 °C. The maximum power is set to 100 W for a compact prototype engine. This work opts for a relatively low charged pressure of 7 bar which also help limiting the size and weight of this prototype. In addition to the containment issues, the safety issue regarding the use of hydrogen is also concerned. As a result, air is selected as the working fluid. For a Stirling engine, there are three basic configurations namely alpha, beta and gamma configurations to choose from. The first consideration is the compactness of the engine package. This aspect rules out the alpha configuration. The gamma configuration yield a slight advantage over the beta configuration in terms of ease of construction due to two separate volumes in which the displacer and the power piston move. The dead volume associated with the connection between the two volumes in gamma configuration, however, compromises the effective expansion temperature and hence the efficiency of the engine [25]. The present work employs the beta configuration.

A first estimation of performance of a Stirling engine is typically obtained from the empirical West equation:

$$W_N = \frac{L_S}{P_m V_{SE} n \left(\frac{T_E - T_C}{T_E + T_C}\right)} \tag{1}$$

The West number, W_N , is 0.35 for engines rated below 5 kW and is 0.25 for engines rated between 5 and 150 kW [26,27]. The performance of developmental engines, however, rarely reached the level prescribed by the West number. However, it can be noticed that, for the design purposes, there is no formal guideline to indicate the running speed required for the use of the West formula.

Iwamoto [28] proposed a method to estimate the output power and the running speed at the same time based on a set of nondimensional parameters. From experimental data of many engines, Iwamoto arrived at two empirical relationships:

$$L^*_{S,\max} = 0.24 n^*_{opt} \tag{2}$$

$$n^*_{opt} = 6.8 \times 10^{-5} S^{*0.6} \tag{3}$$

Table 1
Engine specifications.

Engine type	Beta
Working gas	Air
Maximum charged pressure	7 bar
Displacer: swept volume	165 cc
Displacer: bore × stroke	74 mm × 37 mm
Power piston: swept volume	165 cc
Power piston: bore × stroke	74 mm × 37 mm
Heater section dead volume	20 cc
Heater: design/surface area	Slot/877.8 cm^2
Cooler section dead volume	16.5 cc
Cooler: design/surface area	Slot/708.4 cm^2
Regenerator matrix	#80 Stainless steel mesh
Regenerator porosity	75%
Regenerator section dead volume	47 cc
Compression ratio	1.61
Heating method	Electrical heaters
Cooling method	Water jacket

where n^*_{opt} is the optimum dimensionless engine speed at the condition of the maximum dimensionless output power $L^*_{S,\max}$. As a result, a designer can estimate more accurately the swept volume and the running speed at the same time from a given set of design specifications. Following the method of Iwamoto, the present work arrived at the swept volume for the expansion space at 165 cc and the engine speed of 627 rpm using the design specifications described earlier. The low speed operation translates to the low flow friction loss for the present air charged engine.

From the preliminary sizing of the engine provided by the method of Iwamoto, detailed sizing was performed via the thermodynamic and heat transfer analysis. This work employed the "simple" calculation routine from Urieli [29]. The code involved solving derivative equations describing the flow and energy coming in and out of the different volumes of the Stirling engine. The set of equations allows the simple pressure loss, heat transfer, and indicated power to be determined. As a result, the sizing of the heater, cooler and regenerator volumes can be specified. The final specifications of the engine are provided in Table 1.

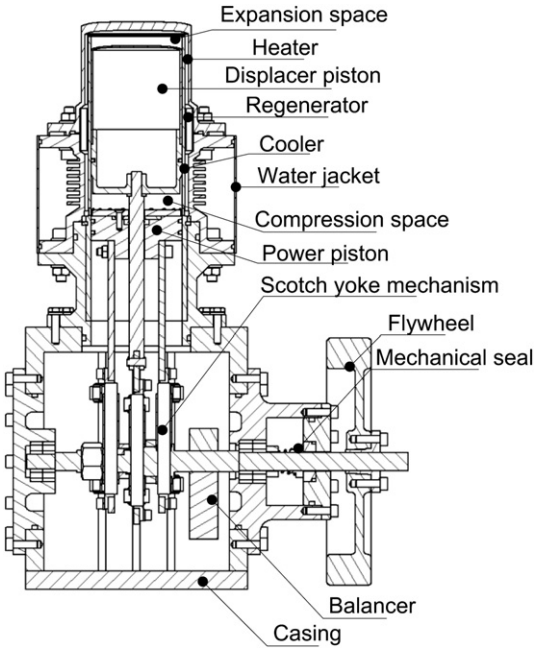

Fig. 1. Details of the Stirling engine.

Fig. 2. The prototype Stirling engine.

3. Engine construction

The engine structure is depicted in Fig. 1. The drive mechanism creates the relative motion of the displacer and power pistons. For the compact construction with reduced side load, the Scotch yoke mechanism was adopted. The mechanism employed standard parts

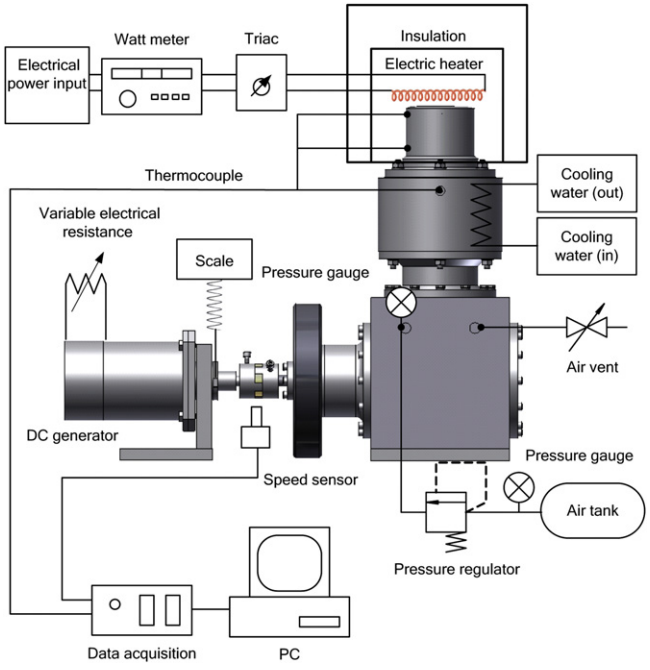

Fig. 3. The measurement system for the Stirling engine.

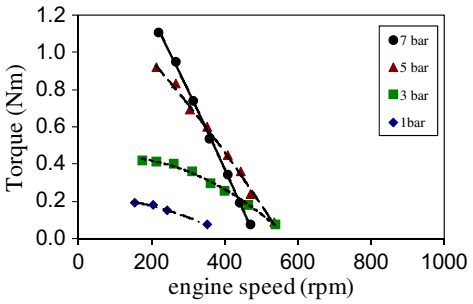

Fig. 4. Torque characteristics for the heater temperature of 350 °C.

such as linear bearing and high speed tool steel rod to minimize built time and development cost. The entire mechanism was designed to run without oil sump.

The design of the displacer for high temperature engines usually has the length to bore ratio of 3–4. For the low temperature difference design, the ratio is less than unity for enhanced heat transfer. For the present work, the ratio is 1.35. For ease of construction and reduced weight and hence inertia force, the displacer is built from aluminum. The clearance space between the displacer and the cylinder liner is 0.5 mm. Due to the moderate temperature difference design; the thermal expansion of the aluminum displacer poses no problem to the engine operation. For the power piston, it must be designed to withstand the pressure difference hence the power conversion from the gas processes. The piston ring must also minimize the leakage through the piston clearance such that the output power is maximized. Designed to work without lubrication, this engine use PTFE piston ring which has the low coefficient of friction and can withstand the temperature up to 300 °C. The clearance between the piston and the liner is 0.04 mm. The cylinder liner is turned from a common steel pipe. The liner bore is surface hardened with nitriding process to ensure long life. For the relative motion between the displacer and power pistons, the cast iron displacer rod is suspended by a brass bush. This combination results in good lubricating properties.

The expansion space above the displacer and the compression space above the power piston are connected by three heat exchanger sections. For compact yet enhanced heat transfer, the slot configuration is selected for the heater and cooler sections. The slots with 3 mm depth and 0.5 mm width are machined along the heater and cooler wall using wire cut technique. The heater section is machined from stainless steel 304 while the cooler section employs aluminum 7075 for enhanced heat conduction to the outside surface. The regenerator matrix consists of #80 stainless steel mesh. The heater section is heavily insulated on the outside using ceramic fiber to minimize heat transfer loss to the environment. The cooler section employed a simple water jacket to dissipate the heat rejected from the engine.

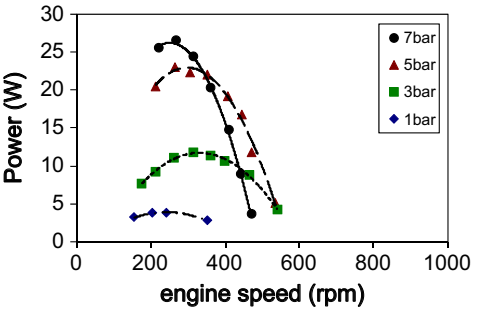

Fig. 5. Power characteristics for the heater temperature of 350 °C.

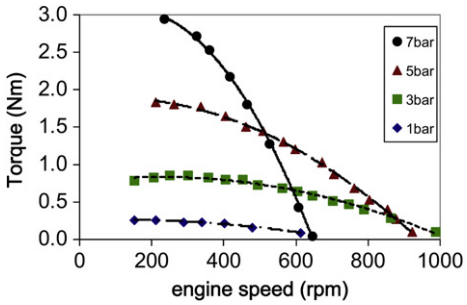

Fig. 6. Torque characteristics for the heater temperature of 500 °C.

The casing is built from aluminum sheet welded together. Although this results in a rather bulky dimension, it is considered optimum choices compared to metal casting considering availabilities of local manufacturing facility and the cost for building the present prototype. For the assembly of engine components, this engine uses synthetic fluorocarbon O-rings for the static seals. These rings are able to withstand up to 300 °C. The only dynamic seal is at the output shaft. The stainless steel and carbon mating parts are chosen for the mechanical seal combination being able to withstand the maximum of 13 bar pressure. The prototype Stirling engine developed in this work is depicted in Fig. 2.

4. Experimental setup and test Procedure

This work attempts to explore the performance of moderate temperature Stirling engine at different values of the charge pressures and wall temperatures at the heater section. The electric heater is employed as a heat source. To simulate the use in solar application, the heater wall temperature is set in between 350 and 500 °C. The heater section including the electric heater is insulated from the environment using layers of ceramic fiber. The input power to the heater is measured using a true rms Watt meter, Yokogawa WT1030. The surface temperatures are measured using type K thermocouples. The charged pressure is provided to the engine via an air compressor with a pressure regulator. The water jacket at the cooler section is supplied to maintain the temperature at the cooler section at 35 °C for all tests. The experimental setup is illustrated in Fig. 3.

The engine is connected to a 120 W DC generator. The generator is connected to an electronic load such that the engine load can be adjusted accurately. To measure the shaft power output, the generator is carried on a cradle such that it is free to rotate. A torque arm attached to the generator provides a measurement of the shaft torque via a calibrated scale. With the running speed available from a tachometer, the shaft power output can be determined.

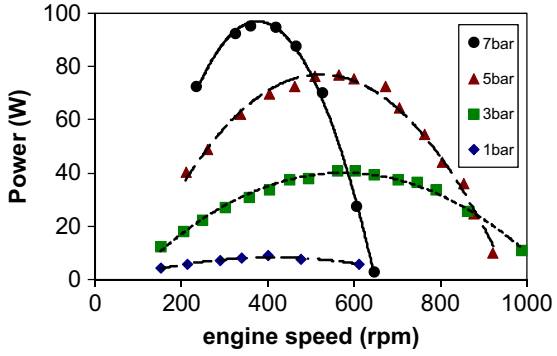

Fig. 7. Power characteristics for the heater temperature of 500 °C.

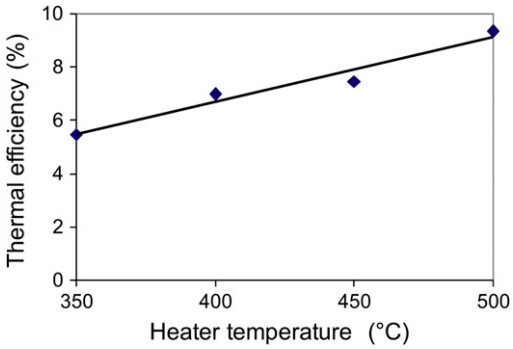

Fig. 8. Variation of the thermal efficiency with the wall temperature at the heater section.

5. Engine performance and analysis

The variations of the engine torque and power with the running speed at different pressures are shown in Figs. 4 and 5 respectively for the heater temperature of 350 °C. The torque in Fig. 4 is at its maximum at the lowest running speed for all charged pressure. This characteristic change of torque with the running speed is typical for Stirling engines [17–21]. From Fig. 5, the engine produces the maximum power of 3.8 W under the atmospheric pressure. The maximum power increases with the increasing pressure and reached the value of 26.6 W at 7 bar.

The corresponding torque and power data for the heater temperature of 500 °C are in Figs. 6 and 7 respectively. By increasing the temperature from 350 to 500 °C, the operating range reaches a much higher speed. It can be noticed that, with increasing charged pressure, the range of the operating speed of the engine increases from 1 to 3 bar and then decreases from 5 to 7 bar. This character can be noticed both in the case of 350 and 500 °C. The maximum torque also increases for up to 50%, i.e. from 1.77 N m to 2.94 N m at 7 bar. At 500 °C and 7 bar, the maximum power reached 95.4 W at 360 rpm.

Fig. 8 shows the maximum thermal efficiency of this engine in terms of the heater temperature. The thermal efficiency is defined as the ratio of the shaft power output to the electrical power input to the electric heater. The data for the charged pressure of 7 bar indicated that the thermal efficiency increased rather linearly with the increased temperature of the heater section and reached 9.35% at the maximum temperature of 500 °C.

To compare the performance of this engine with other studies, the dimensionless West number is depicted in Fig. 9. The West number allows an unbiased comparison of the power output of different machines with different design and operating conditions. The Carnot efficiency is plotted as the *x*-axis to be indicative of the temperature range of the hot end. The data is separated

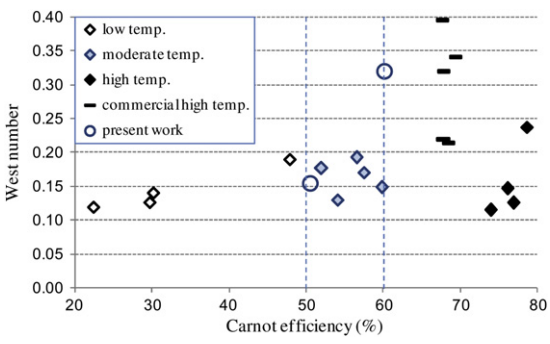

Fig. 9. The West number under different temperature range.

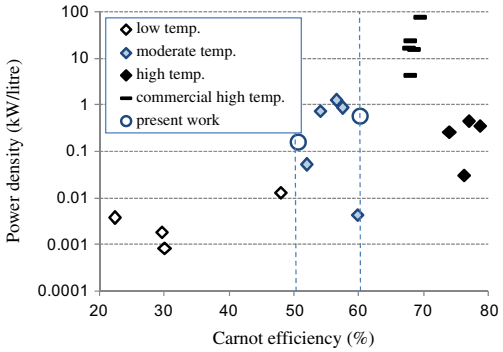

Fig. 10. The power density under different temperature range.

into three groups namely, low, moderate and high temperature difference operations. In addition to the data from academic research, data from the commercial development is also included for comparison. The numerical data and sources are available in Appendix A.

Based on low temperature of 313 K, the moderate temperature range is for the hot end temperature between 350 and 500 °C where the Carnot efficiency is between 50 and 60% respectively. The data showed that the low temperature difference engines offer a rather low value of West number. Operated at higher temperature, Stirling engines obtain the West number in the region of 0.1–0.25 for both moderate and high temperature difference operations. For commercial development, the West number can be as high as 0.4. The present work demonstrated that the moderate temperature difference operations could offer the performance on par with the high temperature operations with more simple and less costly development.

A different way to compare designs of the engines is the specific power. The ratio of the output power over the swept volume of the expansion space over a range of Carnot efficiency is provided in Fig. 10 for the same data as in Fig. 9. The observation from Fig. 10 is quite similar to that from Fig. 9. The moderate temperature operation offers a clear advantage in terms of the specific power over the low temperature operation. The data also show that, with proper design, the moderate temperature operation can be competitive to the high temperature operation.

6. Conclusion and outlooks

The design and performance of a moderate temperature difference Stirling engine are described. The hot end temperature is investigated between 350 and 500 °C. During the design phase, empirical relationships of Iwamoto had proved to be useful. This work opts for low cost design choices including low charged pressure, air working fluid, utilization of standard parts in construction and standard material selection. Under the atmospheric pressure, the engine produces a maximum power of 3.8 W at 205 rpm and 350 °C. At 500 °C and 7 bar charged pressure, the maximum power reached 95.4 W at 360 rpm. At this condition, the thermal efficiency is 9.35%. The dimensionless West number and the specific power demonstrated that the performance of this prototype, in terms of the power output, is on par with the high temperature design with more simple and less costly development. The results of this study indicates the advantage of the moderate temperature design of Stirling engines considering the possibility of developing local know how, utilizing low cost manufacturing and material overhead and employing local workforce.

Acknowledgments

The authors acknowledge the partial funding for this study from the Ratchadaphiseksomphot Endowment Fund, Chulalongkorn University.

Appendix A

The basic data acquired for the production of Figs. 9 and 10 are included here for reference.

	Power (W)	P_m (bar)	V_{SE} (cc)	n (rpm)	T_E (K)	T_C (K)	W_n
Iwamoto [14]	150	1	40200	150	403	313	0.119
Kongtragool [19]	1.69	1	894	52.1	436	307	0.125
Kongtragool [18]	6.1	1	7391	20	*439*	307	0.140
Kongtragool [17]	11.8	1	894	133	589	307	0.189
Ishiki [19]	91	1	1767	500	635	305	0.176
Ecoboy (N2) [30]	60	8	81.4	1155	703	323	0.129
Ecoboy (He) [27]	102	9	81.4	1103	721	313	0.192
Ecoboy (N2) [27]	71	8	81.4	954	737	313	0.170
Kongtragool [17]	32.7	1	7391	42.1	771	310	0.148
Present work, 350 °C	26.63	7	165	267	623	308	0.153
Present work, 500 °C	95.4	7	165	360	773	308	0.320
Basic 400hp [27]	291000	110	17400	452	967	313	0.395
NS-03M [27]	3810	62	161	1401	971	313	0.319
MP1002CA [27]	250	15	59.4	1500	973	313	0.219
NS-03T [27]	4140	64	268.7	1299	991	313	0.214
GPU-3 [27]	8950	69	120	3600	1019	313	0.340
Batmaz [31]	118	2	440	1200	1223	318	0.114
Cinar [32]	128	4	276	891	1273	293	0.125
Cinar [33]	5.98	1	192	208	1273	303	0.146
Karabulut [34]	65	2.5	183	555	1373	293	0.237

References

[1] Ministry of energy. www.eppo.go.th.
[2] Mills A. Advances in solar thermal electricity technology. Solar Energy 2004;76:19–31.
[3] Concentrating Solar Power – From research to implementation. European Commission. Luxembourg: Office for Official Publications of the European Communities; 2007. ISBN 978-92-79-05355-9.
[4] Potentials of Concentrating Solar Power Technologies in Thailand. By Department of Alternative energy development and efficiency, Ministry of energy; 2006.
[5] Newton, C.C. A Concentrated Solar Thermal Energy System. MS Thesis, Mechanical engineering, FloridaState University, (2007).
[6] Yamamoto T, Furuhata T, Arai N, Mori K. Design and testing of the organic Rankine cycle. Energy 2001;26:239–51.
[7] Nguyen VM, Doherty PS, Riffat SB. Development of a prototype low-temperature Rankine cycle electricity generation system. Appl Thermal Eng 2001;21:169–81.
[8] Quiolin, S. Experimental Study and Modeling of a Low Temperature Rankine Cycle for Small Scale Cogeneration. MS Thesis, Electro-Mechanical engineer, University of Liege, (2007).
[9] Peterson, R.B., Wang, H., Herron, T. Performance of a small-scale regenerative Rankine power cycle employing a scroll expander, Proceedings of the Institution of Mechanical Engineers, Part A, 222, (3), (2008), pp.271–282.
[10] http://www.solarturbinegroup.org/field-sites.html.
[11] Tsoutsos T. Technical and economical evaluation of solar thermal power generation. Renewable Energy 2003;28:873–86.
[12] Stirling engine Assessment. Palo Alto, CA: EPRI; 2002. 1007317.
[13] Senft JR. (1991) An ultra low-temperature differential Stirling engine. In: Proceeding of the fifth international Stirling engine conference, paper ISEC 91032, dubrovnik, May 1991.
[14] Iwamoto I., Toda F., Hirata K., Takeuchi M., Yamamoto T. Comparison of low- and high temperature differential Stirling engines. In: Proceedings of the 8th International Stirling Engine Conference, (1997), pp. 29–38.
[15] Kongtragool B, Wongwises S. A review of solar-powered Stirling engines and low temperature differential Stirling engines. Renewable Sustainable Energy Rev 2003;7:131–54.
[16] Tavakolpour AR, Zomorodian A, Golneshan AA. Simulation, construction and testing of a two-cylinder solar Stirling engine powered by a flat-plate solar collector without regenerator. Renewable Energy 2008;33:77–87.
[17] Kongtragool B, Wongwises S. Performance of low-temperature differential Stirling engines. Renewable Energy 2007;32:547–66.
[18] Kongtragool B, Wongwises S. A four power-piston low-temperature differential Stirling engine using simulated solar energy as a heat source. Solar Energy; 2008.

[19] Kongtragool B, Wongwises S. Performance of a twin power piston low temperature differential Stirling engine powered by a solar simulator. Solar Energy 2007;81:884–95 (2007).
[20] Ishiki S, et al. The experimental study of atmospheric Stirling engines using pin-fin arrays' heat Exchangers. J Power Energy Syst 2008;2:1198–208.
[21] Karabulut H, Aksoy F, Ozturk E. Thermodynamic analysis of a beta type Stirling engine with a displacer driving mechanism by means of a lever. Renewable Energy 2008;34:202–8.
[22] Karabulut H, Cinar C, Ozturk E, Yucesu HS. Torque and power characteristics of a helium charged Stirling engine with a lever controlled displacer driving mechanism. Renewable Energy 2009;35.
[23] Tlili I, Timoumi Y, Nasrallah SB. Analysis and design consideration of mean temperature differential Stirling engine for solar application. Renewable Energy 2008;33:1911–21.
[24] Kalogirou SA. Solar thermal collectors and Applications. Prog Energy Combust Sci 2004;30:231–95.
[25] Kearney DW. Parabolic trough collector Overview. Parabolic trough Workshop. NREL; 2007.
[26] Senft JR. Ringbom Stirling engines. New York: OxfordUniversity Press; 1993.
[27] Walker G. Stirling engines. Oxford: Clarendon Press; 1981.
[28] Iwamoto S, Hirata K, Toda F. Performance of Stirling Engines(Arranging method of Experimantal results and performance Prediction). JSME Int Journal Ser B 2001;44(1):140–7.
[29] Urieli I, Berchowitz D. Stirling cycle engine analysis; 1984. Bristol.
[30] Hirata, K., Iwamoto, S., Toda, F. and Hamaguchi, K. Performance evaluation for a 100W Stirling engine. In: Proceedings of 8th International Stirling Engine Conference (ISEC 97003), Ancona, Italy, 1997, pp. 19–28.
[31] Batmaz I, Ustun S. Design and manufacturing of a V-type Stirling engine with double heaters. Appl Energy 2008;85:1041–9.
[32] Cinar C, Karabulut H. Manufacturing and testing of a gamma type Stirling engine. Renew Energy 2005;30:57–66.
[33] Cinar C, Yucesu S, Topgul T, Okur M. Beta-type Stirling engine operating at atmospheric pressure. Appl Energy 2005;81:351–7.
[34] Karabulut H, Yucesu HS, Koca A. Manufacturing and testing of a V-type Stirling engine. Turk J Eng Environ Sci 2000;24(2).

Glossary

L_s: output power (W)
n: engine speed (rpm)
P_m: mean pressure (Pa)
T_E: expansion space temperature (K)
T_c: compression space temperature (K)
V_{SE}: swept volume of the expansion space (m^3)
W_N: West number